analytical chemistry

Article

pubs.acs.org/ac

Single-Shot Analytical Assay Based on Graphene-Oxide-Modified Surface Acoustic Wave Biosensor for Detection of Single-Nucleotide Polymorphisms

Xiang Liu,[†] Jia-Ying Wang,[†,‡] Xiao-Bing Mao,[†,§] Yong Ning,[*,†] and Guo-Jun Zhang[*,†]

[†]School of Laboratory Medicine, Hubei University of Chinese Medicine, 1 Huangjia Lake West Road, Wuhan 430065, China
[‡]Department of Clinical Laboratory, Taihe Hospital, Hubei University of Medicine, 32 South Renmin Road, Shiyan 442000, China
[§]School of Life Sciences, Southwest University, 2 Tian Sheng Road, Beibei, Chongqing 400715, China

Supporting Information

ABSTRACT: The combination of a surface acoustic wave (SAW) biosensor with graphene oxide (GO) provides a promising perspective for detecting DNA mutation. The GO-modified SAW biosensor was prepared by conjugating GO onto the SAW chip surface via electrostatic interaction. Afterward, the probe was immobilized on the GO surface, and detection of DNA mutation was realized by hybridization. The hybridization with a variety of targets would yield different mass and conformational changes on the chip surface, causing the different SAW signals in real time. A total of 137 clinical samples were detected by a single-shot analytical assay based on GO-modified SAW biosensor and direct sequencing in parallel. The diagnostic performance (both sensitivity and specificity) of the assay was evaluated with the direct sequencing as a reference testing method. The phase-shift value of three genotypes in 137 clinical samples was significantly different ($p < 0.001$). Furthermore, testing of diagnostic performance yielded diagnostic sensitivity and specificity of 100% and 88.6% for identifying CT and CC genotype, 98.0% and 96.2% for identifying CT and TT genotype, respectively. The single-shot analytical assay based on the GO-modified SAW biosensor could be exploited as a potential useful tool to identify CYP2D6*10 polymorphisms in clinical practice of personalized medicine.

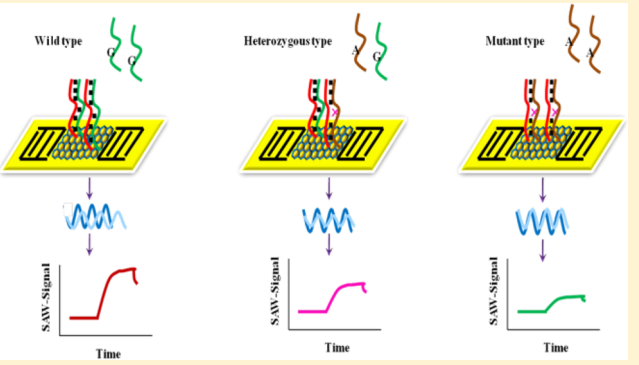

The cytochrome P450 enzyme 2D6 (CYP2D6) plays an important role in the metabolism of 25% of commonly prescribed drugs, such as antipsychotic, antidepressant, antiarrythmia, opiates, and antihypertensive drugs.[1] Genetic polymorphism in CYP2D6 is a crucial factor contributed to interethnic differences in drug response.[2] The CYP2D6*10 allele, a single nucleotide alteration in exon 1 (100C > T), causes a Pro34 → Ser amino acid substitution, leading to an unstable enzyme with lower metabolic activity.[3] CYP2D6*10 is the most common allele in the Chinese population with a frequency ranging from 51 to 70%.[4] Genotype−phenotype correlation studies suggested that accurate genotyping was essential for the implementation of individualized medicine.[5] Therefore, a fast, simple, and economic technique for identifying CYP2D6*10 polymorphisms in the Chinese populations is required for the design of appropriate treatments.

Techniques to identify DNA mutations include direct sequencing, restriction fragment length polymorphism (RFLP), single strand conformation polymorphism analysis (SSCP), reverse hybridization (RH), fluorescence polarization (FP), gel electrophoresis, and mass spectrometry. All of them are reliable but suffer from some disadvantages such as complicated protocols, expense, and time-consuming methods. In recent years, there has been considerable interest in using DNA biosensors based on different transduction principles as flexible, label-free, and rapid tools, and these techniques include aptamer-based electrochemical impedance spectroscopy (EIS) sensors,[6] EIS-based nanostructured biosensor,[7] surface plasmon resonance (SPR) biosensors,[8] SPR imaging (SPRi) DNA sensor,[9] fluorescence biosensor,[10] quartz crystal microbalance (QCM) biosensors,[11] and surface acoustic wave (SAW).[12] Among them, the label-free biosensors based on SAW technology have been developed to detect single-nucleotide polymorphisms (SNPs) as they are extremely sensitive to the mass of the unbound species as well as to viscoelastic properties of the surrounding liquid and layers of bound biological material.[13,14] The new generation of microfluidic SAW sensors has about 4−5 times higher sensitivity than traditional quartz crystal microbalances with dissipation (QCM-D)[15] and can real-time monitor signal changes in standardized systems.[16]

Received: June 4, 2015
Accepted: August 28, 2015

DOI: 10.1021/acs.analchem.5b02121
Anal. Chem. XXXX, XXX, XXX−XXX

This provides a promising perspective for SNP genotyping with high sensitivity and selectivity as well as easy-to-use approaches.

Nanomaterials, such as gold nanoparticles, magnetic nanoparticles, carbon nanotubes, and graphene oxide (GO), play an increasingly important role in the development of biosensors.[13] GO, a single-atom-thick, two-dimensional carbon material prepared by acid exfoliation of graphite,[17] has attracted a growing interest in biological and biomedical applications due to its unique characteristics such as good water-solubility,[18] high carrier mobility,[19] ease of functionalization,[20] and low intrinsic electrical noises.[21] Applied to the DNA-biosensors, GO may improve the sensitivity and selectivity of a sensor because it can increase adsorption of biomolecules through hydrogen bonding and/or $\pi-\pi$-stacking interactions on the interface, making GO a good supporting layer for biomolecules' immobilization.[8] Many investigations have been done to explore the ability of GO as a platform for the sensitive and selective detection of biomolecules. For instance, a GO-assisted SPR biosensor for highly sensitive detection of DNA hybridization has been reported.[8] A novel, simple, sensitive, and selective strategy based on a peptide nucleic acid (PNA)-GO assembled biosensor for fluorescence turn-on detection of DNA has been provided.[22] The study by Liu et al.[23] offers important mechanistic insights into the GO/DNA system, and Lu et al.[24] have suggested the use of GO as a platform for the sensitive and selective detection of DNA and proteins. Wang et al.[25] have described fabrication of a sensitive label-free electrochemical DNA biosensor for the determination of target DNA based on the glassy carbon electrode modified with GO and gold nanoparticles. Another novel electrochemical DNA biosensor based on electrochemical reduced GO and PNA-DNA hybridization has been developed.[26] Very recently, a reduced GO-based field-effect transistor (FET) biosensor used for ultrasensitive label-free detection of DNA via PNA-DNA hybridization has been reported.[27] All these studies collectively indicate that GO, as a valuable nanomaterial, plays an increasingly important role in the development of biosensors. Nevertheless, the combination of SAW with graphene for detecting DNA mutation has never been explored.

Recently, Gronewold and co-workers[28] reported on using a SAW sensor for the highly sensitive and accurate detection of individual point mutations in cancer-related gene DNA fragments. Although reliable and desirable discrimination against a single-base mismatch in DNA target was achieved, the paper neither used a nanomaterial-based sensing interface nor tested their biosensors with PCR-generated targets or real samples. Thus, the result provided only performance features of the SAW sensor in identifying DNA mutations in standard solution but not data of genotype in SNP for real clinical samples, which is more complicated. After all, SNP occurs in human genome at a frequency of approximately 1 in every 1000 bases, not in the known standard fragment.[13] Mazouz et al.[29] developed a 104 MH zlithiumtantalate ($LiTaO_3$) SAW sensor to investigate target-probe recognition processes in only three real samples. Furthermore, the phase shifts were not sufficiently discriminated, probably due to surface functionalization process without spacer. In such a case, the steric hindrance may occur and the sensitivity may decrease. Xu et al.[12] describes a new technique for detecting SNPs by integrating a leaky SAW (LSAW) biosensor, enzymatic DNA ligation and enzymatic signal amplification in attenuated live-vaccine and virulent strains but not in a real clinical sample. Moreover, further enzymatic amplification in this study has an operational complexity and could not meet the requirements of large-scale genotyping.

In this study, we propose a single-shot analytical assay based on GO-modified SAW biosensor for label-free detection of CYP2D6*10 mutation, which is the first example of using the GO-functionalized SAW biosensor for detecting point mutations of drug metabolism enzyme gene. Specifically, this detection system is used to identify CYP2D6*10 polymorphisms in a total of 137 clinical specimens, which is a larger sample size than the previous studies. The results are simultaneously validated by a direct sequencing, a clinical gold standard detection method for SNPs. The developed novel biosensor thus explores the feasibility of the new method, which can be applied to clinical practice.

EXPERIMENTAL SECTION

Reagents and Samples. All chemicals were of analytical grade and were used as received. Natureal graphite, purchased from Alfa Aesar Co., Ltd. (Tianjin, China), was used for synthesis of GO which was prepared by a modified Hummer's method.[30] Cysteamine hydrochloride (cys), 1-ethyl-3-(3-dimethylaminopro-pyl) carbodiimide (EDC), *N*-hydroxysuccinimide (NHS), and ethanolamine (EA) were purchased from Sigma (U.S.A.). Oligonucleotides (Table S1) were obtained from Invitrogen, and ultrapure water was prepared by the Milli-Q System (Billerica, MA, U.S.A.). DNA binding buffer containing 10 mM Tris-HCl, pH 8.3, 1.5 mM $MgCl_2$, 50 mM KCl was also used as running buffer.

Clinical samples came from a total of 137 unrelated Chinese volunteers that gave written informed consent. These Chinese originated from Han nationality, and 88% were born and raised in Hubei Province. They were all healthy volunteers who were recruited during their yearly routine examination at the Huajiahu Hospital of Hubei University of Chinese Medicine. Genomic DNA was extracted from EDTA-anticoagulated blood using the TIANamp Genomic DNA Kit (TIANGEN Biotech Co. Ltd, Beijing). Unless otherwise specified, PCR reagents were adapted all from TIANGEN. The PCR for amplifying 200 bp fragments was performed on a thermocycler (catalog no. 186-1096, Bio-Rad Laboratories, Inc.).

Modification of GO and Immobilization of Probe on the Chip Surface. The process for preparation of the detection chip comprised six steps. (a) The gold surface of the sensor chip was rinsed and sequentially ultrasonicated in water, anhydrous ethanol, and water for a few minutes to remove any adsorbed substances on the surface. (b) The cleaned chip was dried with nitrogen and was immersed in the 10 mM Cys in the dark overnight at room temperature. (c) The chip was rinsed with water, dried with nitrogen, and covered with the diluted GO suspension for 3 h at room temperature. After deposition, washing, and drying, the GO-modified chip was obtained. (d) The carboxyl groups of GO on the chip surface were activated with 1:1 mixture solution of NHS (0.01 $mol \cdot L^{-1}$) and EDC (0.04 $mol \cdot L^{-1}$) for 20 min. (e) An appropriate concentration of probe solution was dropped on the chip and immobilized for 2 h at room temperature. (f) After being carefully in sequence rinsed with water to remove the excessive probe and dried with nitrogen, the chip was incubated in 1 M EA for 20 min at room temperature to deactivate unreacted NHS esters.

SAW-Biosensor Measurements. The sam5 system (SAW Instruments GmbH, Bonn, Germany) was used as the SAW biosensor platform for label-free detection of CYP2D6*10

DOI: 10.1021/acs.analchem.5b02121
Anal. Chem. XXXX, XXX, XXX−XXX

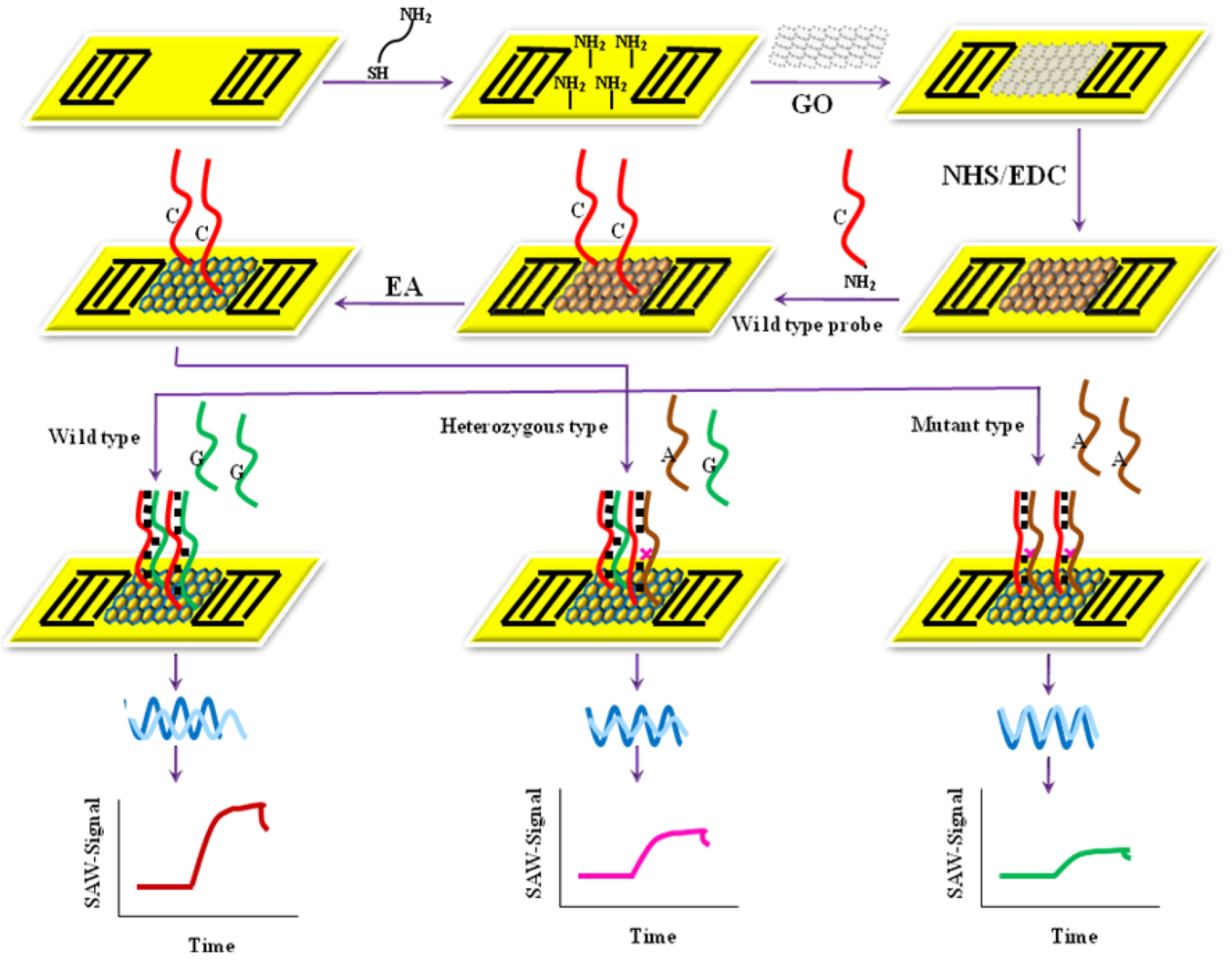

Figure 1. Schematic illustration of the single-shot analytical assay based on GO-modified SAW biosensor for detection of CYP2D6*10 polymorphisms.

mutation online in this study. Calibration and operation procedures were exactly based on the manufacturer's instructions and all experiments were performed at 22 ± 1 °C. Programming and documentation of the experimental conditions were automated by the software packages SensMaster and SequenceMaster.

After the GO and probe at appropriate concentrations were immobilized on the surface of the chip, different target DNA were injected at a flow rate of 40 μL/min and an injection volume of 180 μL, with 200 s total contact time. After each injection, the system was given sufficient time to reach the baseline level by dissociation of the bound DNA in the running buffer. Afterward, the sensor surface was fully regenerated with a pulse of ddH_2O.

Measurement data generated were exported automatically from its SensMaster software into the OriginPro8.1G SR3 (OriginLab, Northhampton, MA), in which the FitMaster was simplified to extract information and to automatize analyses. Because the phase signal is sensitive to both mass changes and viscosity changes and the amplitude signal is influenced almost exclusively by the viscosity effect, the phase signal is recorded and extracted by the software after each injection.[31]

SNPs Analyses of Clinical Samples. The methods for the clinical samples, including direct sequencing and a single-shot analytical assay based on GO-modified SAW biosensors, were carried out in parallel by different operators who were blinded to the results of each other. Sequencing was performed on ABI Prism 3100 (Applied Biosystems, U.S.A.). In the developed method, the purified PCR products were denatured at 95 °C for 5 min and then flash-frozen to yield single DNA chains. The generated ssDNA could be further analyzed by the assay. By applying this protocol, each assay was carried out by using five replicates; all of the data were collected, and the mean phase signal change of each sample was calculated.

Evaluation of Diagnostic Accuracy. Both sensitivity and specificity in diagnostic analysis for the assay based on GO-modified SAW biosensors were calculated and evaluated with the direct sequencing as a reference testing method. Receiver operating characteristic (ROC) curves were then established to evaluate the discriminating effect of CYP2D6*10 polymorphisms of the new method.[32−36] All *P* values were two-sided, and less than 0.05 was considered statistically significant. All statistical analyses were performed using the Statistical Package for the Social Sciences (SPSS 13.0, Chicago, IL).

RESULTS AND DISCUSSION

Detection Principle. The working principle of the single-shot analytical assay based on GO-modified SAW biosensor is

DOI: 10.1021/acs.analchem.5b02121
Anal. Chem. XXXX, XXX, XXX−XXX

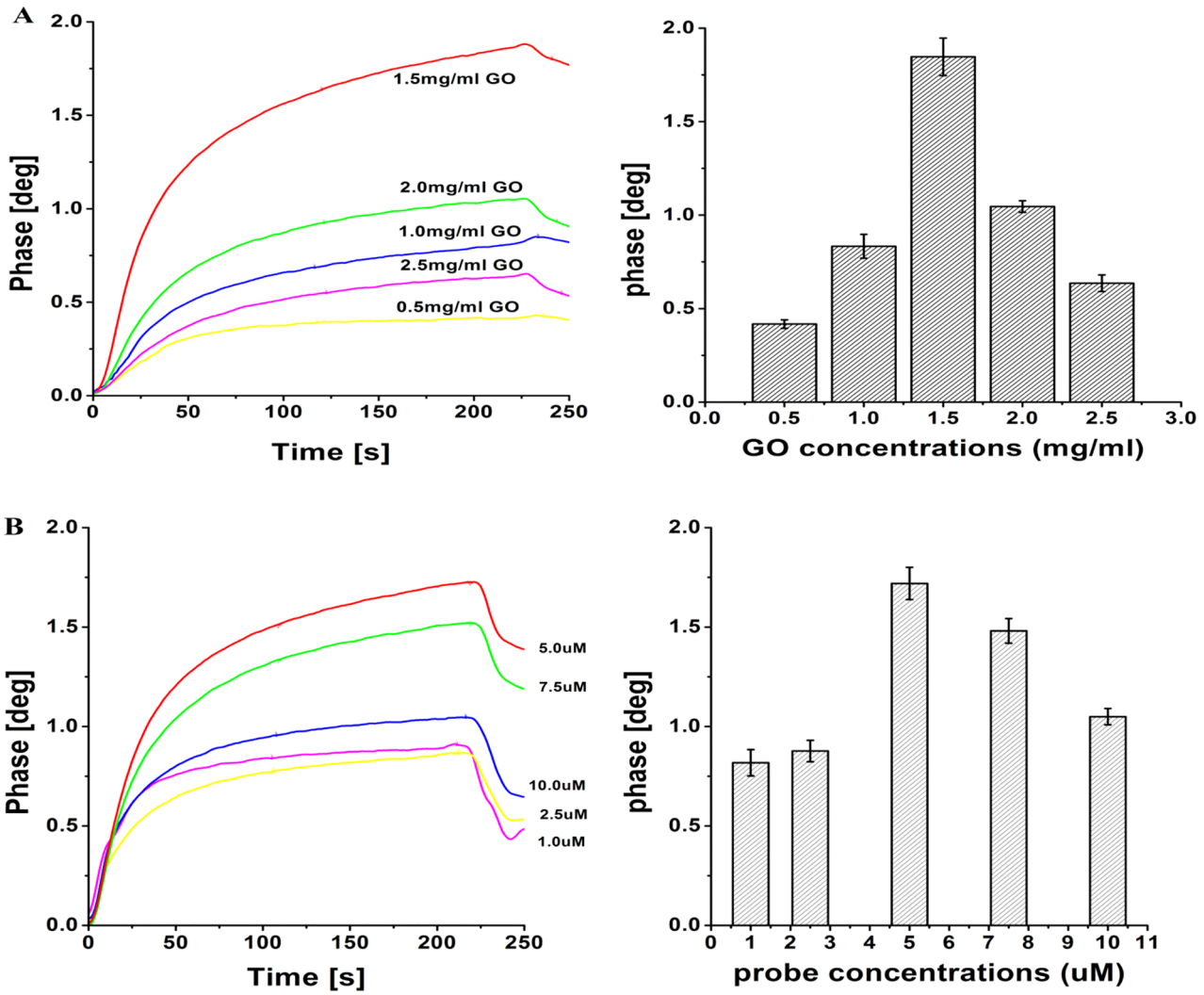

Figure 2. Effect of GO and probe concentration. (A) left: sensing response versus different concentrations of GO; right: bar graph illustrating the effect of different concentrations of GO. (B) left: sensing response versus different concentrations of probe; right: bar graph illustrating the effect of different concentrations of probe.

based on the change in the propagation of a surface acoustic wave within a thin gold film, and the change in phase and amplitude of the propagation wave related to mass deposited on the surface by the biosensor as a result of recognition events occurring between the molecular interactions.[15] The detection principle of the assay based on GO-modified SAW biosensor for detection of CYP2D6*10 polymorphisms is illustrated in Figure 1. First, after the sulfur headgroups of cys bind as thiolates to the gold surfaces of the sensor chip, an aminated self-assembled monolayers (SAMs) forms,[27] resulting in a positively charged interface. Then, the negatively charged GO is easily conjugated onto the positively charged SAMs via electrostatic interaction. Subsequently, the carboxyl groups on the GO surface are activated with a mixture of EDC and NHS and bound to an aminated DNA probe via carboxylamide bonds. Finally, hybridization with a variety of target analytes would yield different mass and conformational changes on the chip surface, causing the different SAW signals monitored by a computer-controlled data acquisition system in real time.

Optimization of Detection Conditions. The sam5 system consisted of five sensor channels. To produce an ideal GO layer, GO of several different concentrations were used to coat the sensing channels. GO, with a final concentration of 0.5, 1.0, 1.5, 2.0, and 2.5 mg/mL, was separately modified on the thin gold film of the five sensor elements, after which the probe (10 μM) was immobilized on the GO layer. The experiment was repeated six times. The concentration which generated maximum phase shift signal was selected as optimal GO coating. It was observed that the phase shift increased when GO concentrations were increased from 0.5 to 1.5 mg/mL. However, the signal decreased when GO concentrations still increased from 1.5 to 2.5 mg/mL. The shift reached the plateau when the GO concentration was 1.5 mg/mL (Figure 2A). The investigation of the optimal concentration revealed that GO concentration substantially affected the hybridization process, which is consistent with the previous investigation.[23] Meanwhile, a Zeiss UltraPlus field emission-scanning electron microscopy (FE-SEM) was used for characterization of the gold surface modified with GO at a 5 kV acceleration voltage. As evident from the SEM image (Figure S1), a few-layer GO sheet spanned across the gold film when 1.5 mg/mL GO was modified on it, whereas the surface was clean on the bare chip surface. The dark color may be ascribed to the folds of the GO. Considering these factors, the optimal GO concentration was determined as 1.5 mg/mL.

DOI: 10.1021/acs.analchem.5b02121
Anal. Chem. XXXX, XXX, XXX−XXX

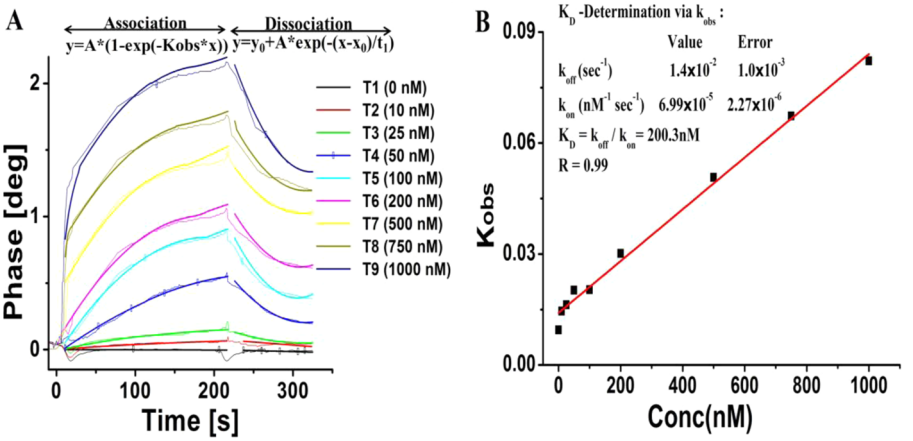

Figure 3. Kinetic analysis of hybridization. (A) Overlay plot and kinetics of FC sequence for different concentrations as indicated. (B) K_{obs} values extracted from the sensor signals and determination of the K_D value.

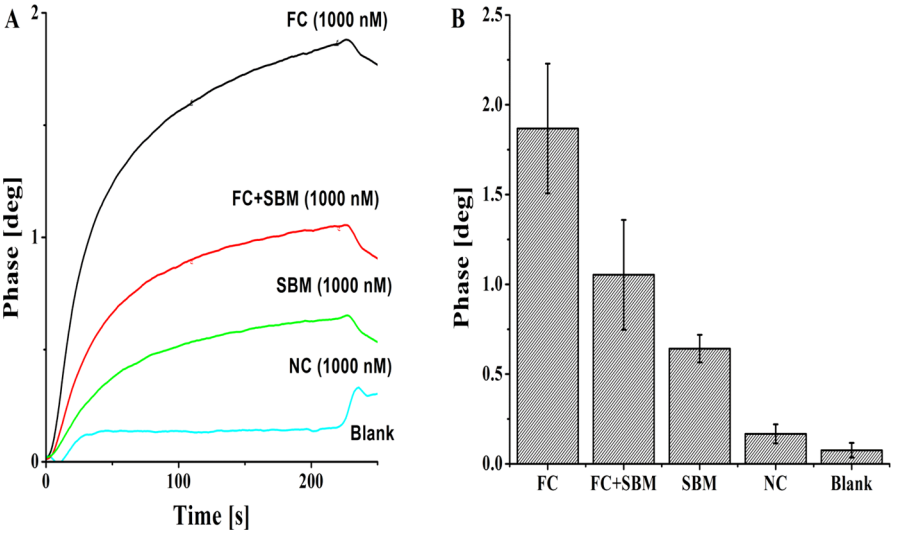

Figure 4. Effect of different configuration. (A) Sensing response versus different configuration. (B) Bar graph illustrating the effect of different configuration.

Probe concentration plays an important role in the detection of hybridization. Similarly, the probes of different concentrations (1.0, 2.5, 5.0, 7.5, and 10.0 μM) were immobilized on the thin gold films of detection channels in order to investigate the appropriate concentration of probe. As demonstrated in Figure 2B, the signal variation first increased along with the DNA probe concentration increase in the range of 1.0 to 5.0 μM, then slightly decreased while the DNA probe concentration continuously increased from 5.0 to 10 μM in the presence of 1.0 μM target DNA. The results showed that 5.0 μM probe produced the highest response, whereas a further increase in probe concentration yielded a reduced response. This is not surprising because probe concentration is related to the surface density of the immobilized probe, which severely governs surface-based DNA pairing due mainly to the steric hindrance and electrostatic repulsion between DNA fragments.[12,37]

Additionally, the performance of all kinds of DNA sensors is critically dependent on the distance (and length of spacer) between biomolecule and sensor surface.[38] Dextran, which can form a hydrogel on top of the sensor surface and provide long and hydrophilic spacer arms, is a commonly used material for signal enhancement in the development of biosensor.[28] To compare the performance of dextran and GO as sensing interfaces, GO and dextran were modified on the chip surface, respectively, and the results were compared. GO and 10 mg/mL dextran were coated on four channels of biosensor, respectively, two for GO and the others for dextran. In the following steps, only one among the two channels was immobilized by the probe. After the oligonucleotide was injected, SAW signals of each channel were recorded. Figure S2 highlighted that the GO layer had slightly higher background signal than the dextran one, but the layer (GO + probe) produced significantly higher phase shift value than the one (dextran + probe). Moreover, the ratio of the signal, defined as $(\text{signal}_{M+probe} - \text{signal}_M)/\text{signal}_M$ (M is GO or dextran), was 4.16 for GO, which is higher than 3.01 for dextran. This indicates that GO is more suitable than dextran as the sensing interface, probably because of unique characteristics of GO as above-mentioned. Because the GO matrix can provide larger surface area and more functional groups, it might accumulate more biomolecules on the interface, which may affect the propagation of the surface acoustic wave by a physical pattern, such as the change of mass and viscosity on a deposited layer.[15]

Kinetic Analysis of Hybridization. To determine the association and dissociation kinetics of the target fragments to

DOI: 10.1021/acs.analchem.5b02121
Anal. Chem. XXXX, XXX, XXX−XXX

Table 1. Figures of Merit of Commercially Available and of Recently Developed Methods for Detecting Polymorphism

method/material used	LOD	specific applicability and merits	ref
fluorescence: F-2500 fluorometer (Hitachi, Japan) equipped with an aqueous thermostat (Amersham) accurate to 0.1 1C.	40 fM	detection of SNP of β-thalassemia gene at position 28 using ligation-rolling circle amplification and stemless molecular beacon	10
EIS: SP-150 potentiostat (Bio-Logic), the gold thin film-coated nanostructured electrode	/	efficient detection of the haplotype of two SNPs in the group 2 allergens gene promoter	7
electrochemical: Voltalab 40 PGZ 301 system consisting of silicon nitride working electrode, a saturated calomel reference electrode, and a platinum auxiliary electrode	100 nM	unambiguous discrimination of SNP of ApoE in real clinical genotypes	25
SPR: SPRi-Lab+ and SPRi-Biochips glass prisms coated with gold from Horiba Scientific (France)	0.18 fM	direct detection of C3435T SNP in human multidrug resistance gene on the unamplified human DNA extracted from lymphocytes	9
LSAW: the LSAW biosensor was obtained from the 26th Research Institute, Chinese Electronic Scientific and Technical Group Company	1pM	detection of SNP at nucleotide A2293G in Japanese encephalitis virus strains by enzymatic DNA ligation and enzymatic signal amplification	12
SAW: AW Instruments GmbH, Bonn, Germany	86.5 pM	detection of CYP2D6*10 SNP in 137 clinical samples with diagnostic sensitivity and specificity of 100% and 88.6% for identifying CT and CC genotype, 98.0% and 96.2% for identifying CT and TT genotype	this work

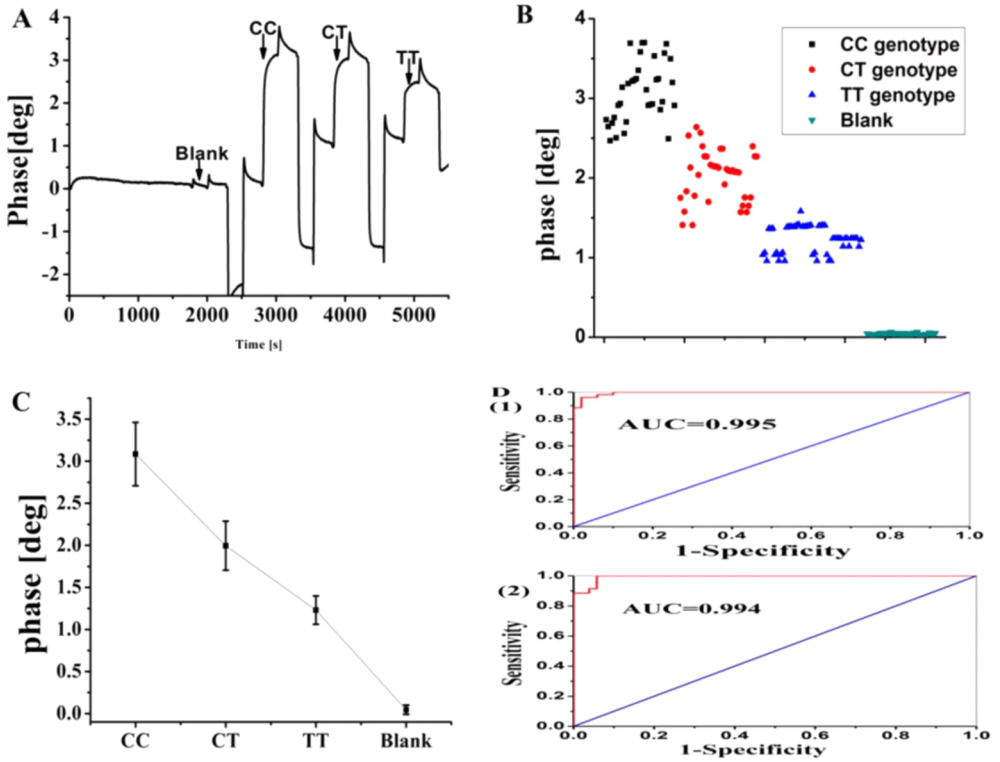

Figure 5. Detection of SNPs at CYP2D6*10 by the single-shot analytical assay based on GO-modified SAW biosensors. (A) Online detection of clinical samples. (B) Plots of phase-shift values for different genotype from 137 clinical samples. (C) Comparison of the signals among three genotypes of 137 clinical samples. (D) ROC curve analysis using the single-shot analytical assay based on GO-modified SAW biosensor for discriminating CYP2D6*10 polymorphisms: (1) An AUC of 0.994 (95% confidence interval (CI): 0.984−1.000; $P < 0.0001$) with 100% sensitivity and 88.6% specificity in identifying CT and CC genotype; (2) An AUC of 0.995 (95% CI: 0.988−1.000; $P < 0.0001$) with 98.0% sensitivity and 96.2% specificity in identifying CT and TT genotype.

the immobilized probe, the fully complementary (FC) oligonucleotides of increasing concentrations (0 nM to 1000 nM) were injected to the probe-immobilized sensors successively. The changes of the sensor phase signals were fitted with Origin software in the monomolecular growth model and the exponential decay model. The phase shift in increasing concentrations and corresponding fitting curves for FC sequence at every concentration, including the equations used for calculating association and dissociation kinetics, was shown in Figure 3A. Association and dissociation were fitted under the assumption of a 1:1 binding model using the origin-based FitMaster program. The pseudo-first order kinetic constants K_{obs} as determined by the FitMaster were plotted versus the concentrations in Figure 3B. A linear fit was applied using the equation shown. The average k_{off} [Unit in sec^{-1}] equals the intersection with the y-axis. The slope of the fitted straight line is a measurement of the k_{on} rate [unit in $conc^{-1}$ s^{-1}]. The K_D value is calculated with $K_D = k_{off}/k_{on}$. The binding of FC sequence yielded a fitted K_D value (dissociation equilibirum constant) of about 200.3 nM, which is similar to the results in the previous research.[28] Linear regression presented a good linear range from 10 nM to 100 nM with a correlation coefficient of $R = 0.99$ and a standard deviation of <0.001. Kinetic evaluations give insight into how well the mobile FC sequence was bound to the immobilized probe, indicating that the system is suitable for real-time dynamic

DOI: 10.1021/acs.analchem.5b02121
Anal. Chem. XXXX, XXX, XXX−XXX

detection of DNA hybridization in the certain concentration range.

Selectivity and Sensitivity of the Single-Shot Analytical Assay Based on GO-Modified SAW Biosensor. Due to the significance of the sensor selectivity, especially in SNP assays, the discrimination capability of this single-shot analytical assay by using FC sequence (similar to CC wild-type specimens), single-base mismatch (SBM, similar to TT mutant-type specimens) sequence, the 1:1 mixture of FC and SBM (FC + SBM, similar to CT heterozygous-type specimens) and noncomplementary (NC, similar to nonspecific fragment specimens) sequence, as well as blank control, respectively, was investigated. The concentrations of all target sequences were 1.0 μM. As shown in Figure 4, the sequences could be readily distinguished from each other. It was noticed that the FC sequence exhibited prominent signals, whereas signals corresponding to all other oligonucleotides decreased successively. This is probably because the phase shifts are mainly related to mismatch nature and position. CA mismatch pair designed at the middle position of strand is easily distinguishable with the lowest hybridization rate.[29] The data do confirm that the SAW biosensors are of high specificity and can be used in SNP assays.

To determine the sensitivity and the limit of detection (LOD) of this approach, the optimized system was employed to challenge with a series of FC DNA concentrations. Figure 3A represented the typical signal across the concentration range from 0 to 1000 nM. It was found that a linear relationship between the phase variation (Y) and the logarithmic value of target DNA concentration (10 to 1000 nM) with a regression equation ($Y = 0.982 \log[C(\mathrm{nM})] - 0.959$, $R^2 = 0.991$, $n = 5$) (Figure S3) were obtained. LOD was calculated to be 86.5 pM based on the $3\sigma/S$ calculation (σ is the standard deviation of the blank signal, and S is the slope of the calibration curve, $n = 20$), whereas the biosensor showed an excellent response at >10 nM target DNA concentration. Compared with other DNA detection techniques (Table 1), the LOD of the present assay was lower than the electrochemical sensor but higher than the EIS-, SPRi-, and LSAW-based sensors. As known, both electrochemical and fluorescent assays require tags, which is not a direct detection scheme. The result of high sensitivity achieved by SPRi was mainly dependent on the SPR imaging dual-targeting DNA assay, together with the combination of the rational selection of the DNA probe and an optimized sample pretreatment.[9] Although the LSAW-based sensor also provided a lower LOD, effective enzymatic DNA ligation and enzymatic signal amplification should be required. It is obvious that these methods suffer from the complicated detection procedures. Hence, the present method is simple and direct, allowing for the determination of genotype in clinical samples without additional thermal elevation, stringency washes, or the use of time-consuming signal amplification.

SNPs Analysis of Clinical Samples. CYP2D6*10 allele as detection target was selected on the basis of its important role in individualized medicine and the popularity in Chinese population. By a direct sequencing (Figure S4), a total of 35 samples (25.5%) were characterized as CC wild-type, 52 as CT heterozygous-type (38.0%), and 50 as TT mutant-type (36.5%). According to the results, the frequency of CYP2D6*10 allele was 55.5%, which is comparable to the previous data in Chinese,[2] suggesting that the clinical samples used in this study are appropriate.

All 137 clinical samples were detected by the assay based on the GO-modified SAW biosensor. The corresponding online-detection diagram of CC, CT, and TT genotype determined by sequencing is presented in Figure 5A. Each dot (except blank control) in Figure 5B represented the mean phase-shift value of five replicates from each clinical sample and was categorized as CC, CT, or TT genotype on the basis of results from the direct sequencing. Comparison of the signals at different genotype of 137 clinical samples was indicated in Figure 5C. The mean phase-shift value (range) was found to be 3.09 (2.96−3.22) with an SD (standard deviation) of 0.38 for CC genotype, 1.99 (1.91−2.08) with an SD of 0.29 for CT genotype, and 1.23 (1.18−1.28) with an SD of 0.16 for TT genotype. The phase signals of three genotypes were significantly different ($p < 0.001$), and change tendency was similar to the above selectivity test, except for the increased signal intensity possibly owing to enhanced mass of clinical samples.

To estimate diagnostic accuracies of the assay based on GO-modified SAW biosensor, sensitivity, specificity, and the area under the curve (AUC) were determined using ROC analysis. At the cutoff value of 2.64, the sensitivity and the specificity were 100% and 88.6% for identifying CT and CC genotype with an AUC of 0.994 (95% CI: 0.984−1.000; $P < 0.0001$), respectively (Figure 5D(1)). Applying the same model and cutoff value to 1.49, the testing samples yielded an AUC of 0.995 (95% CI: 0.988−1.000; $P < 0.0001$) with 98.0% sensitivity and 96.2% specificity, indicating the discriminating effect of CT and TT genotype (Figure 5D(2)). These results reveal that the assay based on GO-modified SAW biosensor could serve as valuable means for differentiating CT heterozygous-type from CC and TT homozygous-type of CYP2D6*10. Unlike the previous reports not sufficiently discriminating the phase shifts in real sample[29] or not sensitive enough to detect SBM without further enzymatic amplification,[12] we have demonstrated that the system is able to differentiate CYP2D6*10 polymorphisms without using the strategy of signal amplification and/or labeling. The fact is probably due to high sensitivity and an efficient software-driven access for automated sample processing and data analysis of the GO-based SAW biosensor.

CONCLUSIONS

In summary, the single-shot analytical assay based on GO-modified SAW sensor for simple, rapid, and sensitive detection of CYP2D6*10 polymorphisms in clinical samples have been explored. More importantly, these promising results with high sensitivity and specificity could be seen as the starting point for later work oriented toward the clinical application. Of course, to further validate the diagnostic performance of the new method, additional testing must be performed in other genotypes of the CYP2D6 SNP, as well as other SNP. Furthermore, the detection system still leaves room for improvement in some approaches such as PCR-free for sample pretreatments, multiplicity analysis using five sensor elements, and other protocols. Nevertheless, the developed system shows outstanding performance of label-free detection and rapid response as a single-shot analytical assay platform, which may represent a useful new tool for identification of SNP in clinical practice of personalized medicine.

ASSOCIATED CONTENT

Supporting Information

The Supporting Information is available free of charge on the ACS Publications website at DOI: 10.1021/acs.analchem.5b02121.

DOI: 10.1021/acs.analchem.5b02121
Anal. Chem. XXXX, XXX, XXX−XXX

Detailed descriptions of oligonucleotides used in this study, SEM image of the gold chip surface, comparison of GO and dextran, a linear relationship between the phase variation and the logarithmic value of target DNA concentrations, and detection of SNPs at CYP2D6*10 by direct sequencing (PDF)

AUTHOR INFORMATION

Corresponding Authors

*E-mail: zhanggj@hbtcm.edu.cn. Tel.: +86-27-68890259. Fax: +86-27-68890071.
*E-mail: ningyong128@163.com.

Notes

The authors declare no competing financial interest.

ACKNOWLEDGMENTS

This work was supported by China Postdoctoral Science Foundation to X.L. (No. 2014M552023) and Natural Science Foundation of China (Nos. 21275040 and 21475034).

REFERENCES

(1) Bradford, D. L. *Pharmacogenomics* **2002**, *3*, 229−243.
(2) Johansson, I.; Oscarson, M.; Yue, Q. Y.; Bertilsson, L.; Sjoqvist, F. *Mol. Pharmacol.* **1994**, *46*, 452−459.
(3) Paar, W. D.; Poche, S.; Gerloff, J.; Dengler, H. J. *Eur. J. Clin. Pharmacol.* **1997**, *53*, 235−239.
(4) Samer, C. F.; Piguet, V.; Dayer, P.; Desmeules, J. A. *Can. J. Anaesth.* **2005**, *52*, 806−821.
(5) Dahl, M. L.; Yue, Q. Y.; Roh, H. K.; Johansson, I.; Sawe, J.; Sjoqvist, F.; Bertilsson, L. *Pharmacogenetics* **1995**, *5*, 159−164.
(6) Chen, X.; Huang, Y.; Ma, X.; Jia, F.; Guo, X.; Wang, Z. *Microchim. Acta* **2015**, *182*, 1709−1714.
(7) Chin, Y. T.; Liao, E. C.; Wu, C. C.; Wang, G. J.; Tsai, J. J. *Int. J. Nanomed.* **2014**, *9*, 1403−1412.
(8) Zagorodko, O.; Spadavecchia, J.; Serrano, A. Y.; Larroulet, I.; Pesquera, A.; Zurutuza, A.; Boukherroub, R.; Szunerits, S. *Anal. Chem.* **2014**, *86*, 11211−11216.
(9) Mariani, S.; Scarano, S.; Carrai, M.; Barale, R.; Minunni, M. *Anal. Bioanal. Chem.* **2015**, *407*, 4023−4028.
(10) Zou, Z.; Qing, Z.; He, X.; Wang, K.; He, D.; Shi, H.; Yang, X.; Qing, T.; Yang, X. *Talanta* **2014**, *125*, 306−312.
(11) Sun, L.; Frykholm, K.; Fornander, L. H.; Svedhem, S.; Westerlund, F.; Akerman, B. *J. Phys. Chem. B* **2014**, *118*, 11895−11904.
(12) Xu, Q.; Chang, K.; Lu, W.; Chen, W.; Ding, Y.; Jia, S.; Zhang, K.; Li, F.; Shi, J.; Cao, L.; Deng, S.; Chen, M. *Biosens. Bioelectron.* **2012**, *33*, 274−278.
(13) Chang, K.; Deng, S.; Chen, M. *Biosens. Bioelectron.* **2015**, *66*, 297−307.
(14) Ponder, B. *Science* **1997**, *278*, 1050−1054.
(15) Gronewold, T. M. *Anal. Chim. Acta* **2007**, *603*, 119−128.
(16) Cui, J.; Iturri, J.; Götz, U.; Jimenez, M.; del Campo, A. *Langmuir* **2013**, *29*, 6582−6587.
(17) Kim, K. S.; Zhao, Y.; Jang, H.; Lee, S. Y.; Kim, J. M.; Kim, K. S.; Ahn, J. H.; Kim, P.; Choi, J. Y.; Hong, B. H. *Nature* **2009**, *457*, 706−710.
(18) Liu, Z.; Robinson, J. T.; Sun, X.; Dai, H. *J. Am. Chem. Soc.* **2008**, *130*, 10876−10877.
(19) Mohanty, N.; Berry, V. *Nano Lett.* **2008**, *8*, 4469−4476.
(20) Huang, Y.; Dong, X.; Shi, Y.; Li, C. M.; Li, L. J.; Chen, P. *Nanoscale* **2010**, *2*, 1485−1488.
(21) Lin, Y. M.; Avouris, P. *Nano Lett.* **2008**, *8*, 2119−2125.
(22) Guo, S.; Du, D.; Tang, L.; Ning, Y.; Yao, Q.; Zhang, G. J. *Analyst* **2013**, *138*, 3216−3220.
(23) Liu, B.; Sun, Z.; Zhang, X.; Liu, J. *Anal. Chem.* **2013**, *85*, 7987−7993.
(24) Lu, C. H.; Yang, H. H.; Zhu, C. L.; Chen, X.; Chen, G. N. *Angew. Chem., Int. Ed.* **2009**, *48*, 4785−4787.
(25) Wang, Z.; Zhang, J.; Yin, Z.; Wu, S.; Mandler, D.; Zhang, H. *Nanoscale* **2012**, *4*, 2728−2733.
(26) Du, D.; Guo, S.; Tang, L.; Ning, Y.; Yao, Q.; Zhang, G. J. *Sens. Actuators, B* **2013**, *186*, 563−570.
(27) Cai, B.; Wang, S.; Huang, L.; Ning, Y.; Zhang, Z.; Zhang, G. *ACS Nano* **2014**, *8*, 2632−2638.
(28) Gronewold, T. M.; Baumgartner, A.; Quandt, E.; Famulok, M. *Anal. Chem.* **2006**, *78*, 4865−4871.
(29) Mazouz, Z.; Fourati, N.; Zerrouki, C.; Ommezine, A.; Rebhi, L.; Yaakoubi, N.; Kalfat, R.; Othmane, A. *Biosens. Bioelectron.* **2013**, *48*, 293−298.
(30) Kovtyukhova, N. I.; Ollivier, P. J.; Martin, B. R.; Mallouk, T. E.; Chizhik, S. A.; Buzaneva, E. V.; Gorchinskiy, A. D. *Chem. Mater.* **1999**, *11*, 771−778.
(31) Pohl, A.; Weiss, I. M. *Beilstein J. Nanotechnol.* **2014**, *5*, 1823−1835.
(32) Boyd, J. C.; Rifai, N.; Annesley, T. *Clin. Chem.* **2012**, *58*, 1273−1274.
(33) Linnet, K.; Bossuyt, P. M.; Moons, K. G.; Reitsma, J. B. *Clin. Chem.* **2012**, *58*, 1292−1301.
(34) Moons, K. G.; de Groot, J. A.; Linnet, K.; Reitsma, J. B.; Bossuyt, P. M. *Clin. Chem.* **2012**, *58*, 1408−1417.
(35) Reitsma, J. B.; Moons, K. G.; Bossuyt, P. M.; Linnet, K. *Clin. Chem.* **2012**, *58*, 1534−1545.
(36) Bossuyt, P. M.; Reitsma, J. B.; Linnet, K.; Moons, K. G. *Clin. Chem.* **2012**, *58*, 1636−1643.
(37) Yang, F.; Yang, X.; Wang, Y.; Qin, Y.; Liu, X.; Yan, X.; Zou, K.; Ning, Y.; Zhang, G. J. *Anal. Chem.* **2014**, *86*, 11905−11912.
(38) Ocaña, C.; del Valle, M. *Microchim. Acta* **2014**, *181*, 355−363.

DOI: 10.1021/acs.analchem.5b02121
Anal. Chem. XXXX, XXX, XXX−XXX